

Porcine reproductive and respiratory syndrome virus (PRRSV) preferentially infected the apical surface of primary endometrial cell monolayer

Muttarin Lothong¹ Suphot Wattanaphansak²

Chatsri Deachapunya³ Sutthasinee Poonyachoti^{1*}

Abstract

The underlying mechanism of porcine reproductive and respiratory syndrome virus (PRRSV) causing reproductive failure and re-circulation in herds has remained unclear. Endometrial cells primarily infected with PRRSV may serve as a significant target for PRRSV eradication. Primary endometrial (PE) cells from the porcine uterus were isolated and cultivated to pursue this possibility. Immunocytochemistry analysis revealed the protein expression of classical estrogen receptors (ER- α and ER- β), but not PRRSV receptors, CD163 and sialoadhesin in PE cells. PE cells were apically/basolaterally inoculated with PRRSV type I/type II isolated from PRRSV infected lungs or mock infection. Cytopathic effects (CPE) and PRRSV-GP5 positive cells were detected in PE cells incubated with PRRSV inoculum (10^7 TCID₅₀/ml) beginning at 4 days post inoculation (dpi). Only apical inoculation produced effects, suggesting route dependence of PRRSV infectivity in PE cells ($p<0.05$). PRRSV type II produced overall effects i.e., CPE, PRRSV-GP5 positive cells and a viral load higher than type I ($p<0.05$) during 2-6 dpi. In accordance with these effects, the tissue epithelial resistance (TER) of type II inoculated PE cells was lower than that of mock or type I inoculated cells ($p<0.05$). In addition, all the PE cells and media samples collected from PRRSV-inoculated PE cells persistently revealed PRRSV-GP5 protein and viral copies (10^2 - 10^8 TCID₅₀/ml) accessed by infecting MARC-145 cells. These findings provided the first evidence that PE cells can be directly infected with PRRSV, favorably by type II at the apical side. However, all PRRSV contaminated PE cells persistently carry the progeny virus.

Keywords: Endometrial cells, Porcine reproductive and respiratory syndrome, PRRSV receptor, Releasing of virus, Susceptibility

¹Department of Physiology, Faculty of Veterinary Science, Chulalongkorn University, Henri-Dunant Rd., Pathum Wan, Bangkok 10330, Thailand

²Department of Veterinary Medicine, Faculty of Veterinary Science, Chulalongkorn University, Henri-Dunant Rd., Pathum Wan, Bangkok 10330, Thailand

³Department of Physiology, Faculty of Medicine, Srinakharinwirot University, Sukhumvit Rd., Watthana, Bangkok 10110, Thailand

*Correspondence: sutthasinee@gmail.com (S. Poonyachoti)

Introduction

Porcine reproductive and respiratory syndrome (PRRS) is an important disease in pigs caused by an enveloped single positive stranded RNA virus which belongs to the Arteriviridae family (Snijder and Meulenbergh, 1998; Dokland, 2010). Two genotypes of PRRS virus (PRRSV) have been mainly characterized, type I (EU; Lelystad virus (LV) strain) and type II (US; VR-2332 virus strain) (Nelsen *et al.*, 1999). Infection with PRRSV type I and type II results in reproductive failure in sows and gilts (late-term abortions, stillbirths, and mummies), respiratory failure in all ages of pigs and a high mortality rate in weaning pigs.

Besides horizontal transmission, vertical transmission of PRRSV by shedding of virus from dams to fetus during pregnancy appears to be the major cause of abortion and weak-born piglets that serve as a reservoir of PRRSV (Rossow *et al.*, 1996). To date, the underlying mechanism and the pathogenesis of PRRSV-induced reproductive failure remain unclear. It has been suggested that macrophages and endothelial cells surrounding the implantation sites are associated with PRRSV infection (Karniychuk and Nauwynck, 2009; Karniychuk *et al.*, 2011). Due to the tropism of PRRSV, infected macrophages are believed to be the PRRSV carrier as Trojan mechanisms and spread PRRSV throughout fetal-maternal implantation site of the endometrium and placental membrane. Nevertheless, whether the endometrium and placenta can be the direct target site for PRRSV infection or serve as reservoirs of PRRSV is still questioned.

Indeed, infection with PRRSV is limited to some types of cells that express the specific PRRSV receptors. In natural PRRSV infection, only two mediators, sialoadhesin/CD169 (Sn/CD169) and CD163, have been identified on pulmonary alveolar macrophage (PAM) and are predominant PRRSV receptors for PRRSV infection and replication in target cells (Van Breedam *et al.*, 2010). However, the expression of these PRRSV receptors and the target cells of PRRSV infection in the reproductive tissues has not yet been identified.

In the nasal epithelial cell explants, PRRSV exploits its receptors to enter host cells, and successively replicates inside the host cell within 72 h. post inoculation. The airway epithelial cell barrier seems to be resistant to the type I, but not the type II (Frydas *et al.*, 2013). However, the different virulence of reproductive failure caused by different genotypes of PRRSV remains unclear. Also, dysfunction in PRRSV-infected cells related to the pathogenesis of reproductive disorders is not clearly explained. Only a few apoptotic cells have been indicated at the implantation site uniting fetal/maternal membrane of PRRSV-inoculated sows (Karniychuk and Nauwynck, 2013). It is possible that the damaged epithelia in the PRRSV-infected host might impact the microenvironment and predispose to other infections because the barrier is compromised. This evidence may cause improperly nourished fetuses during the pregnancy, leading to late-term abortion in PRRSV-infected sows.

Endometrium, the mucosal inner layer of the uterus consists of 2 types of epithelial cells, the luminal

and the glandular epithelia. The progressive invagination of luminal epithelia leads to the generation of glandular epithelia, which plays an important role in secretory function, conceptus survival and implantation (Filant and Spencer, 2014). Apart from reproductive function, endometrial cells are involved in an innate immunity. The lining of endometrial epithelial cells and the secretion of several factors act as a physical and chemical barrier to prevent the pathogen invasion of tissues (Lorenzen *et al.*, 2015). In addition, endometrial cells have been focused as the site of virus infection, replication and spreading, such as human and bovine herpes viruses, that leads to virus-induced reproductive failure (Donofrio *et al.*, 2008; Caselli *et al.*, 2017).

Possibly, porcine endometrium is one of the PRRSV infection, replication and spreading sites by occupying PRRSV specific receptors. To gain insight into this information, the expression of PRRSV receptors associated with the susceptibility of endometrial cells to PRRSV infection, replication and spreading were investigated *in vitro* using porcine primary endometrial (PE) epithelial cell culture. The electrical properties of PE cells, the tissue epithelial resistance and potential difference were also assessed to reflect the epithelial barrier and cell polarity which maintain a suitable microenvironment during normal time and pregnancy. This study, like virtually all *in vitro* studies, provided the first evidence of the direct effects of PRRSV infection in the porcine glandular endometrium which simulates the natural membrane of the placental layer.

Materials and Methods

Materials: Drugs and chemicals were purchased from Sigma Chemical Co., (USA). Chemicals used for cell culture consisting of Dulbecco's modified Eagle's medium (DMEM), Dulbecco's phosphate buffer saline (PBS), fetal bovine serum (FBS), collagenase type I, 0.25% trypsin/EDTA, penicillin-streptomycin and fungizone were purchased from GIBCO BRL (USA). All cell culture vessels were purchased from Corning (USA).

PRRSV viral isolation: PRRSV infected lungs of weaned pigs aged between 4 and 8 weeks were obtained from the Farm Animal Hospital, Faculty of Veterinary Science, Chulalongkorn University, Nakorn Pathom, Thailand where sows experienced severe respiratory infection and reproductive failure. PRRSV infection was confirmed by virus isolation following Meng and co-workers' protocol (Meng *et al.*, 1996). Briefly, the infected lung tissue (2.3 g) was minced and homogenized in 15 ml of cold FBS-free DMEM. The homogenate was centrifuged at 10,000 g at 4°C for 10 mins, and the supernatant was collected and filtered through a 0.2 µm syringe. The filtrate was diluted at 1:1 with FBS-free DMEM and freshly used as inoculum for this study.

In order to ensure the infectivity of the viral inoculum, all lung isolated inoculum was determined using MARC-145 cells, the standard PRRSV permissive cells, according to the protocol of Ding *et al.* (2012). Briefly, 10⁵ of MARC-145 cells (ATCC, USA) were

seeded and cultured in maintaining media (5% FBS in DMEM with 100 U/ml penicillin and 100 µg/ml streptomycin). At confluent, MARC-145 cells were incubated with PRRSV inoculum at 37°C in 5% CO₂ for 1 h. Tenfold serial dilutions, 10⁻¹ to 10⁻⁵ of the viral inoculum, were performed to access the virus titer. Cytopathic effects (CPE) in each MARC-145 cell culture well were observed microscopically for 4 days. The TCID₅₀/ml endpoint dilution of lung isolated PRRSV inoculum that produced CPE by 50% of inoculated MARC-145 cells assay was determined using the Reed-Muench method (Reed and Muench, 1938). To confirm the existence of PRRSV particles, some cells were subsequently fixed in 4% paraformaldehyde for immunocytochemistry.

To assess the PRRSV genotypes and concentration, the total RNA from all inoculum were isolated by Multiplex RT-qPCR commercial kit (Accessquick™, Promega, USA), using primers N26: GCCCTAATTGA ATAGGTGAC; FT1: AGAAAAAGAAAAGTACAGC TCCGAT and N26/FT2.1: GTGAGCGGCAATTGTGT CTGT CG respectively, specific to ORF7 of type I / type II, ORF 7 of type I and ORF 7 of type II, respectively. Based on the manufacturer's protocol, 3 µg of cDNA template was mixed in qPCR SYBR mastermix in the presence of forward and reverse primers. The PCR program starting with 95°C for 3 mins to activate the reaction, followed by 40 cycles of amplification steps including denaturation at 95°C for 20 secs, annealing at 60°C for 30 secs and extension at 72°C for 30 secs respectively. The specificity of amplification products was confirmed by performing 1.5% agarose gel electrophoresis and melting curve analysis. During the amplification, the numbers of cycles initially detecting the emission of SYBR green that incorporated into PCR product of each sample were recorded and reported as threshold cycle (*C_t*).

Standardization of a recent Multiplex RT-qPCR kit, viral inoculum at *C_t* = 35 was equivalent to 2.0x10⁴ PRRSV copies per microliters (Liu *et al.*, 2013). The *C_t* of PRRSV Type I and Type II inoculum was calculated from the standard curve suggested by the previous study (Liu *et al.*, 2013). Thus, based on the microtitration in MARC-145 cells and the Multiplex RT-qPCR assay, the approximate viral concentration of inoculum used in the present study was a 10⁷ TCID₅₀/ml. In addition, the inoculum contaminated with *Mycoplasma spp.* and classical swine fever virus as confirmed by Multiplex RT-qPCR, was excluded from the study.

Porcine primary cell isolation and culture: Porcine uterine tissues of 4-6 months pigs were obtained from a governmental qualifying slaughterhouse in Bangkok, Thailand. During transportation, the uterine tissues were kept in ice-cold porcine Ringer solution (NaCl 130 mM, KCl 6 mM, CaCl₂ 3 mM, MgCl₂ 0.7 mM, NaHCO₃ 20 mM, NaH₂PO₄ 0.3 mM and Na₂HPO₄ 1.3 mM; pH 7.4). Primary porcine endometrial (PE) cells were isolated following our previous protocol (Deachapunya and O'Grady, 1998), that had been characterized and tested for functional activity. Briefly, the uterine tissues were cut and washed in Ca²⁺- and Mg²⁺- free PBS. The stripped mucosal layer was minced and digested overnight with 0.2%

collagenase. Endometrial glands were collected from the digested tissues by filtration (40 µm pore size) followed by gravitational sedimentation. The pellets were resuspended and cultured in a 100 mm cell culture dish with maintaining media until confluent (5% FBS in DMEM added with 100 U/ml penicillin, 100 µg/ml streptomycin, 100 µg/ml kanamycin, 1% non-essential amino acids and 10 µg/ml insulin at 37 °C in 5%CO₂). PE cells were trypsinized and sub-cultured to the appropriate cell culture vessels for the experiments. PE cells contaminated with *Mycoplasma spp.*, swine fever virus or PRRSV were excluded when they were positive to the Multiplex RT-qPCR detection kit (Microplasma 16s Ribosomal RNA Gene genesig® Standard kit, Primerdesign, Camberley, UK; Viotype® CSFV RT-PCR kit, QIAGEN, Germany; Viotype® PRRSV RT-PCR kit, QIAGEN, Germany).

The purity of the porcine glandular epithelial cell culture was over 98% as determined by the immunocytochemistry staining of anti-pan cytokeratin antibody and a high tissue epithelial resistance (Deachapunya and O'Grady, 1998). PE cells expressing TER about 400-800 Ω.cm² were considered confluent and chosen for inoculation.

PRRSV inoculation to PE cells: To examine the routing effect of PRRSV transmission, PE cells (10⁶) were plated and maintained in 24 mm microporous membranes for 7 days. The confluent PE cell monolayers were either apically or basolaterally incubated with 2 ml (10⁷ TCID₅₀/ml) of solution isolated from PRRSV type I-positive lung, PRRSV type II-positive lung, or PRRSV-negative lungs (mock infection) for 1 h at 5% CO₂, 37°C. Each infection was done in duplicate from 5 pigs. After incubation, the cells were washed and replaced with the fresh media. At 2, 4 and 6-day post infection (dpi), the membrane-grown inoculated PE cells showed the CPE under light microscope with digital camera (BX50F and UC50, Olympus, Japan) and were fixed in 4% paraformaldehyde to perform immunocytochemistry.

To determine the PRRSV releasing to media, the cultivated medium (200 µl) from apical and basolateral side of infected PE cells was collected at 2, 4 and 6 dpi. The fresh culture media were replaced with the same volume. The collected samples were stored at -70 °C for virus titration by inoculating MARC-145 cells as described above. All results were reported as the average viral titers value (TCID₅₀/ml) determined at 2, 4 and 6 dpi from 5 pigs.

RNA extractions and reverse transcription: Viral RNA samples for multiplex RT-PCR were extracted from the viral inoculum, infected PE cell (10⁶) and cultivated media using TRIzol® reagent (Invitrogen™, USA). According to the manufacturer's instruction, the cultivated PE cells were trypsinized with 0.25% trypsin/EDTA and centrifuged to collect cells. Pellets which were then lysed by 200 µl of TRIzol® reagent. Chloroform 40 µl were added and centrifuged at 12,000 g, 4°C for 15 min (Micro Centaur Plus, MSE, UK) to separate nucleic acid from contaminant. Total RNA was collected from the transparent layer of sample and precipitated in 100 µl of isopropanol. The RNA pellet was collected after centrifugation and washed with

75% ethanol in diethylpyrocarbonate (DEPC). The final total RNA pellets were air dried and dissolved in 20 μ l nuclease-free water (Bio-rad, Inc., USA). Total RNA concentration was measured at an optical density (OD) 260 nm using NanoDrop equipment (NanoDrop 2000c, Thermo Fisher Scientific, USA), and purity was determined by calculation of the OD_{260/280} ratio. The RNA sample was accepted when the ratio was between 1.8 and 2.0.

The first strand DNA was synthesized by reverse transcription using cDNA synthesis kit (iScriptTM, Bio-rad, Inc., USA). According to the manufacturer's protocol, total RNA 3 μ g was mixed with 20 μ l of cDNA synthesis reaction containing 2 μ l Oligo dT primer, 4 μ l 5x iScript reaction mix, 1 μ l iScript reverse transcriptase and nuclease-free water. The reaction was transformed to cDNA using TGradient thermocycler (Biometra, Germany) using the following cycle 25°C for 3 mins, 46°C for 20 mins, and 95°C for 1 min. The cDNA product was stored at -20°C until performing multiplex RT-qPCR.

Determination of electrical properties of PE cells: PE cells (2.5×10^5) were seeded and maintained on 12 mm microporous membrane for 7 days. Tissue epithelial resistance (TER) and potential difference (PD) were measured using transepithelial volt-ohmmeter (MillicellERS-2, Merck KGaA, Germany) before and at 2, 4 or 6 days after PRRSV inoculation. Each value of TER and PD was measured in triplicate from 5 pigs.

Immunocytochemistry and cytopathic effect analysis: The confluent PE cells were determined for expression of PRRSV receptors (CD163 and Sn) by immunocytochemistry. In brief, the cells grown on membrane were fixed in 4% paraformaldehyde for 10 mins at room temperature and washed with PBS. The sample membranes (n=5 pigs) were then incubated with 10% H₂O₂ in methanol and 4% goat serum in PBS to block non-specific binding followed by overnight incubation with primary antibodies for PRRSV receptors or estrogen receptors at 4°C. Each primary antibody was diluted with 1% BSA and 0.1% tween in PBS to obtain the dilution as follows: 1:25, goat-anti-CD163 (Santa Cruz biotechnology, Santa Cruz, USA); 1:250, mouse-anti-sialoadhesin (Serotec®, Bio-rad, Inc., USA); 1:250, mouse-anti-ER- α and 1:250, mouse-anti-ER- β (Santa Cruz biotechnology, Santa Cruz, USA). To detect PRRSV, the membranes were incubated with rabbit polyclonal antibody against PRRSV envelop glycoprotein GP5 at a dilution of 1:100 (Biorbyt Ltd., UK) at 4°C for 4 h. The diluent without primary antibody was used as a negative control. After incubation, the membranes were washed with 0.1% tween in PBS and incubated for 1 h. with the biotinylated secondary antibodies conjugated with horseradish peroxidase (HRP) 1:200, donkey-anti-goat (Santa Cruz biotechnology, Santa Cruz, USA) or 1:2000, mouse-anti-mouse/rabbit IgG (Vectastain, Vector laboratories, Inc., USA) followed by avidin-biotin-enzyme complex (Vector Labs) incubation for 30 mins at 25°C. DAB (3,3-diaminobenzidine tetrahydrochloride) were added, and counterstained with hematoxylin (Histostain-SP, Invitrogen, USA). After the final wash, the stained membranes were

mounted on a glass slide with cover slip on mounting solution (Histostain®, Invitrogen, USA), and the images were observed and captured under light microscope connected with a digital camera (BX50F and UC50, Olympus, Japan).

The dark-brownish color of each sample was determined and subtracted from the non-specific background in negative control (5 fields/sample). The data were reported as the positive immunoreactivities. The positive results of PRRSV-GP5 expression in PE cells were confirmed by comparing the positive control using PRRSV-inoculated MARC-145 cells. The presence of CPE was observed and measured in the same field of observation (5 fields/sample). All of the images were measured at a magnification of 20x and analyzed by image processing program (ImageJ, NIH, USA). The area of CPE was further calculated and reported as % CPE area/field. The measured area of immunoreactive cells was calculated and reported as means of % immunoreactivity/field from n=5 pigs. All experiments were done in triplicate for each pig.

Data analyses: All data obtained in three independent experiments from at least five different PE cells isolated from 5 pigs was expressed as mean \pm SEM. The effects of strains and routes of infection on the expression of PRRSV and CPE as well as the effects of strains and time on the electrical properties of PE cells were statistically analyzed using Analysis of Variance (ANOVA). The difference between the treatments, or compared to the mock, following a significant ANOVA, was identified by Newman-Kuel or Dunnett's test when appropriated. A *p* value of less than 0.05 was considered a significant difference using Graphpad Prism 5.0 (Graphpad software Inc., USA).

Results

Expression of PRRSV and estrogen receptors by primary porcine endometrial cells: At day 7 of cultivation on microporous membrane, PE cells had epithelial-like shape, organized lining and were confluent. The dark-brown areas shown in Fig. 1 (*Upper panel*) represented cellular immunoreactivities of PRRSV and ER receptors. The cellular expression of CD163 and Sn was rarely observed at 0.94 \pm 0.59% and 2.41 \pm 1.01% immunoreactivity/field, respectively, while that of ER- α and ER- β was dominantly demonstrated in PE cells at 37.74 \pm 1.01% and 30.93 \pm 4.20% immunoreactivity/field, respectively. The ER- α immunoreactivity was located in the areas surrounding the nucleus, whereas the ER- β immunoreactivity was revealed in both cytoplasmic and nuclear regions (Fig. 1, *Upper panel*).

Cellular expression of PRRSV-GP5 associated with microscopic changes of PE cells by PRRSV inoculation: In the present study, the positive control of isolated PRRSV from the lungs of PRRSV-inoculated pigs was performed in MARC-145 cells. Inoculation of MARC-145 cells with supernatant containing PRRSV type I or type II collected from PRRSV-infected lungs revealed the dark-brownish color of PRRSV-GP5 immunoreactivity which was apparently observed in all infected cells starting at 2 dpi compared to the mock

(Fig. 2). Moreover, focal degeneration areas or loss of cells were widely observed in MARC-145-inoculated cells with PRRSV type I or type II (Fig. 2), indicating the suitability of lung-isolated PRRSV pathogenicity used for the rest of study.

In the PE cells, however, PRRSV-GP5 immunoreactivity could not be detected until 4 dpi. As shown in Fig. 2, the PRRSV-GP5 immunoreactivity was intensely revealed inside the PE cells when inoculated at the apical side of the monolayer at 4 dpi with PRRSV type I or type II. However, the intensity gradually decreased toward 6 dpi. PRRSV-GP5 could not be detected in PE cells that were inoculated with mock or basolaterally inoculated with PRRSV type I and type II at any observed time (Fig. 2).

Corresponding to PRRSV-GP5 immunoreactivity at 4 dpi, CPE was present in all PRRSV-infected PE cells, but not in the mock group (Fig. 2; $p<0.05$). The accumulation of PE cells carrying PRRSV proteins was demonstrated by syncytial formation as observed in apically PRRSV type I inoculated cells (Fig. 2). Likewise, PE cells inoculated apically with type II produced CPE, to a great extent, the degenerative foci in particular. Consistent with the PRRSV-GP5 existence, all PE cells basolaterally inoculated with PRRSV showed normal cell morphology which was not different from the mock group during 2-6 dpi (Fig. 2).

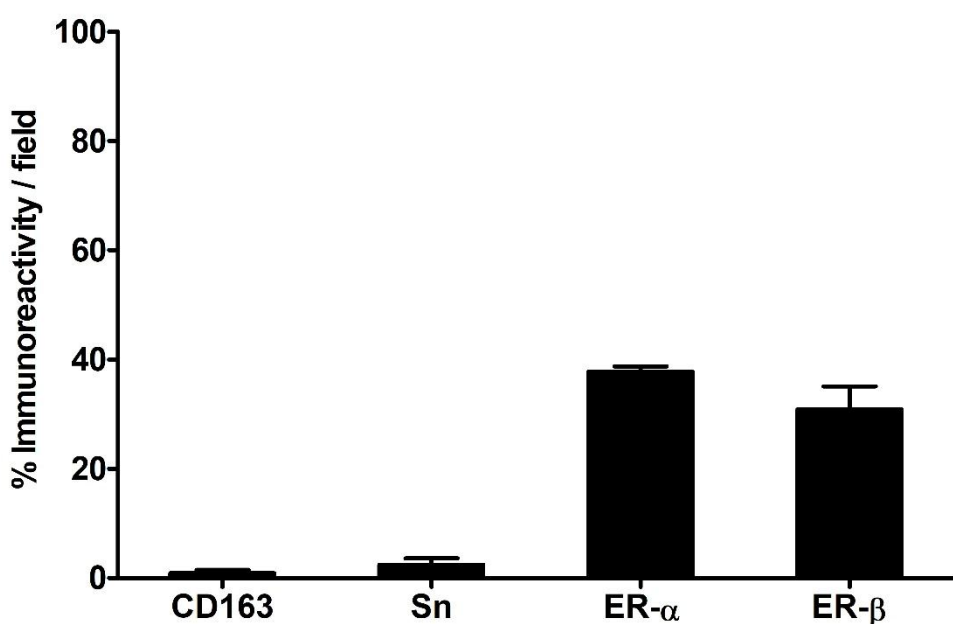
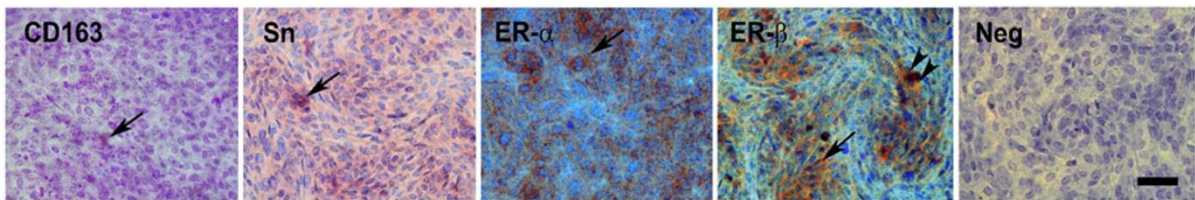


Figure 1 Characterization of glandular epithelia and PRRSV receptors in PE cells observed under light microscope. The upper panel shows the micrograph of the immunocytochemistry staining of anti-CD163, Sn, ER- α and ER- β antibodies in microporous membrane-grown PE cells prior to PRRSV inoculation (at 0 dpi). The dark-brown color represents positive immunoreactivity located at the cytoplasmic (arrow) or nuclear (arrowheads) region. The negative control (Neg) by omitting the primary antibodies shows no immunoreactivity. The Scale bar = 500 μ m. The lower panel shows mean \pm SEM of % immunoreactive area / field of CD163, Sn, ER- α and ER- β in PE cells observed over 5 fields (n=5 pigs).

To compare the overall different effect of route and strain of PRRSV infection, the average percent of area of PRRSV-GP5 immunoreactivity and CPE produced during 2-6 dpi were quantitated and analyzed in Fig. 3.

Concerning basolateral inoculation, little to no expression of PRRSV-GP5 immunoreactivity was detected in PRRSV-inoculated PE cells (Fig. 3A; type I; $0.00\pm0.00\%$ and type II; $0.85\pm0.20\%$). However, a small but significant increase in CPE (Fig. 3B; type I and type II; $5.24\pm0.60\%$ and $6.74\pm1.20\%$, respectively) was

detected in basolateral PRRSV-inoculated PE as compared to the mock (Fig. 3B; $p>0.05$).

On the other hand, when apically inoculated, both type I and II could enter the PE cells as evidenced by the findings that more than 20% of PE cells obviously expressed PRRSV-GP5 proteins during 2-6 dpi (Fig. 3A). The average area of PRRSV-GP5 immunoreactivity following the apical inoculation of type I was significantly higher than that of type II (Fig. 3).

3A, type I $27.35 \pm 3.23\%$ and type II $34.92 \pm 2.75\%$; $p < 0.05$).

A quantitative analysis of the average CPE area produced by different routes and strains of isolated PRRSV during 2-6 dpi indicated that the apical PRRSV inoculation produced a CPE area about 20-30% per

field which was higher than those of basolateral inoculation ($< 10\%$ per field; Fig. 3B; $p < 0.001$). Furthermore, the presence of CPE by PE cells apically inoculated with PRRSV type II ($33.04 \pm 3.50\%$) was higher than cells with PRRSV type I inoculation (Fig. 3B; $18.07 \pm 2.50\%$; $p < 0.001$).

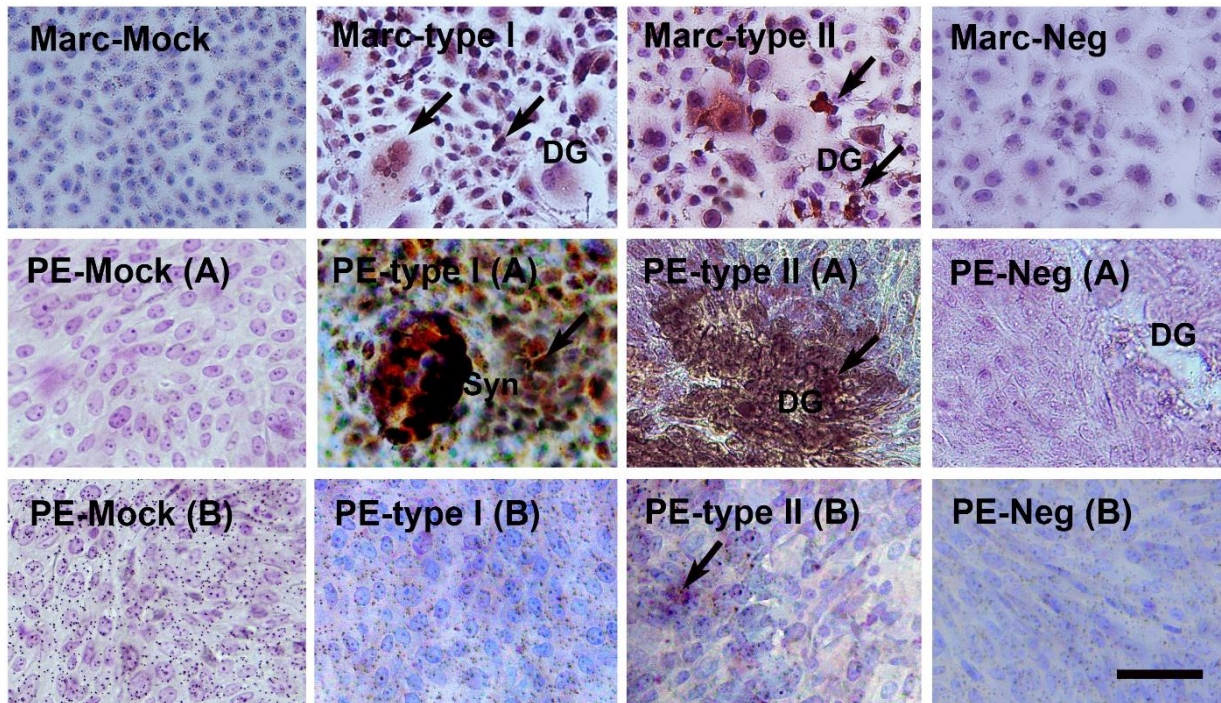


Figure 2 Detection of cytopathic effect (CPE) and expression of PRRSV-GP5 in PRRSV-inoculated MARC-145 and PE cells. The micrograph represents immunocytochemistry staining of anti-PRRSV-GP5 antibody in MARC-145 cells inoculated with mock (Marc-Mock), type I (Marc-type I) or type II (Marc-type II)-PRRSV isolated from the lungs of pigs at 4 dpi. The immunocytochemistry staining of anti-PRRSV-GP5 antibody was also observed in PE cells inoculated at the apical side with PRRSV type I (PE-type I (A)), type II (PE-type II (A)) or mock (PE-Mock (A)). No immunoreactivity was detected in PE cells inoculated at the basolateral side with mock (PE-Mock (B)), PRRSV type I (PE-type I (B)) or type II (PE-type II (B)), and all primary antibody omission control (Marc-Neg, PE-Neg (A) and PE-Neg (B)). The dark-brown color (arrow) represents positive immunoreactivity. The presence of CPE characterized by syncytial formation (Syn) and degeneration (DG) was demonstrated in PRRSV-inoculated MARC-145 or PE cells. Scale bar = $500 \mu\text{m}$.

PRRSV release by PRRSV-inoculated PE cells: To further confirm the characteristic of PE cells in promoting viral release, the culture media collected from PRRSV-inoculated PE cells every 2 days was taken to incubate MARC-145 cells, and the presence of CPE and PRRSV-GP5 protein was evaluated by immunocytochemistry. MARC-145 cells incubated with media collected from either the apical or basolateral side of PRRSV type I or type II-inoculated PE cells demonstrated about 10-40% PRRSV immunoreactive cells on average during 2-6 dpi (Fig. 4). Overall, PE cells inoculated with PRRSV type II, either apically or basolaterally, generated an average viral release higher than PRRSV type I-inoculated cells as evidenced by high immunoreactivity in MARC-145 cells (Fig. 4; $p < 0.005$).

In contrast, no positive immunoreactivity was detected in MARC-145 cells incubated with media obtained from mock inoculated PE cells (Fig. 4; Mock). Instead, the presence of cell degeneration (DG) was detected only in MARC-145 cells inoculated with media collected from PE cells inoculated basolaterally with PRRSV type II (Fig. 4; upper panel).

Determination of PRRSV titers in PE-inoculated cells and PE-inoculated media: Since the viral existence was detected in all PE cells and their culture media, the PRRSV titers were further measured following the Reed-Muench method (Reed and Muench, 1938). As shown in Fig. 5, the highest average of viral load ($\geq 10^8$ TCID₅₀/ml) was detected in PE cells and culture media inoculated with PRRSV type II at the apical side during 2-6 dpi as compared to the mock ($p < 0.05$). However, the apical infection with PRRSV type I generated viral replication and release at an average concentration of 10^6 - 10^7 TCID₅₀/ml ($p < 0.05$). It is notable that all basolateral infection with PRRSV had the lowest viral load in PE cells and media with the viral concentration of $\leq 10^3$ TCID₅₀/ml ($p < 0.05$). Dissimilarly, the culture media collected from basolateral PRRSV-infected PE cells had a viral load higher than other samples of basolateral infected route, even though it was not as much as the apical infected route (Fig. 5; 10^4 TCID₅₀/ml; $p < 0.05$). Neither type I nor type II viral RNA was detected in the PE cells or culture media with mock infection at any time point.

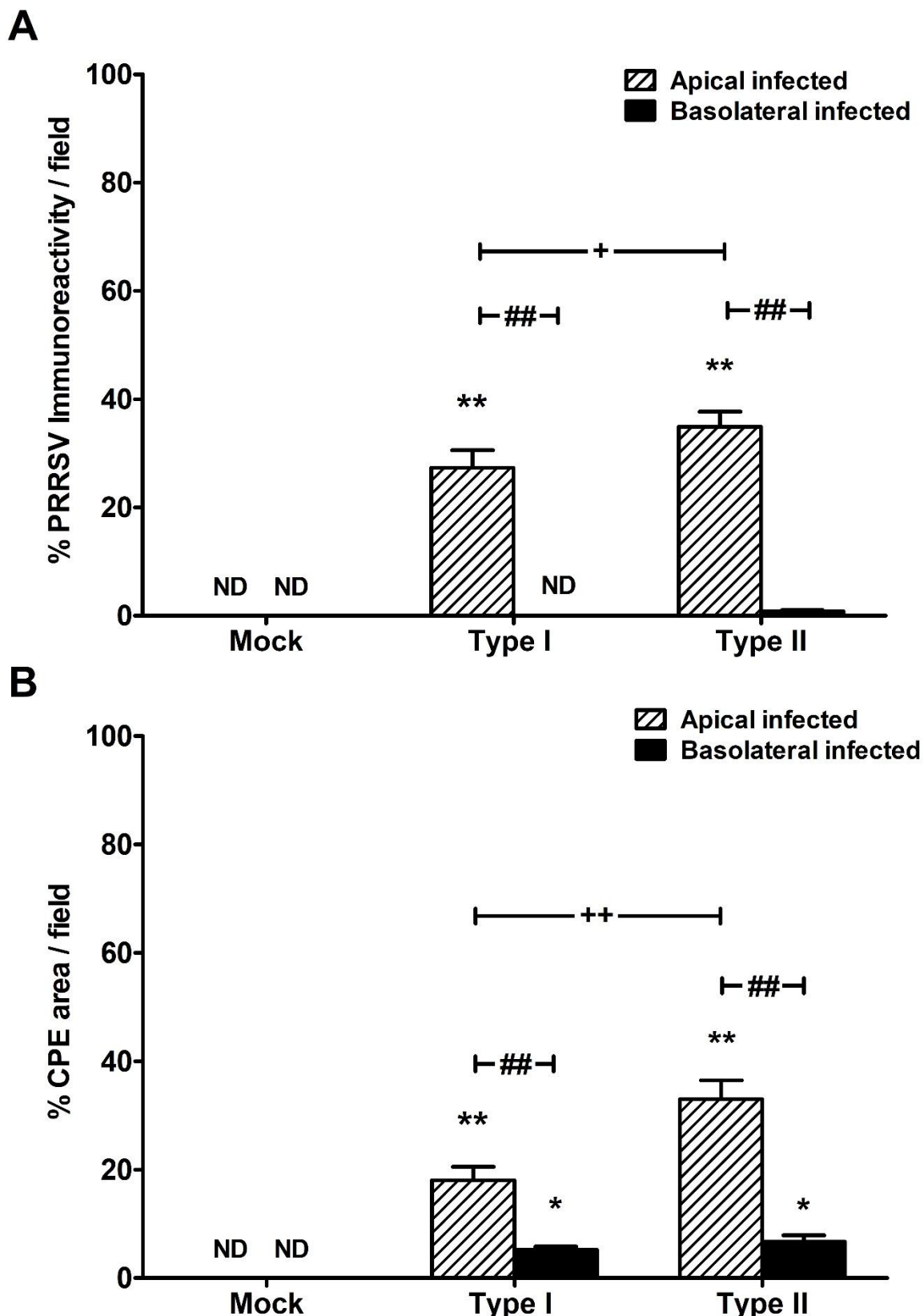


Figure 3 Susceptibility of PE cells to PRRSV inoculation determined by PRRSV-GP5 protein expression and cytopathic effects (CPE). The cells were apically or basolaterally inoculated with mock, PRRSV type I or type II for 1 h. The average immunoreactivity area in response to anti PRRSV-GP5 antibody and CPE in PRRSV-inoculated PE cells was measured and demonstrated as (A) % PRRSV immunoreactivity/field or (B) % CPE/field. Bar graph shows mean ± SEM (n = 5 pigs) recorded at 2, 4 and 6 dpi. * or ** indicates the significant differences at p value <0.05 or <0.01 from mock, ## or ++ respectively indicates the significant differences between routes of inoculation, and between strains at $p<0.01$ by two-way ANOVA followed by Bonferroni post-hoc test. ND=Non-detectable.

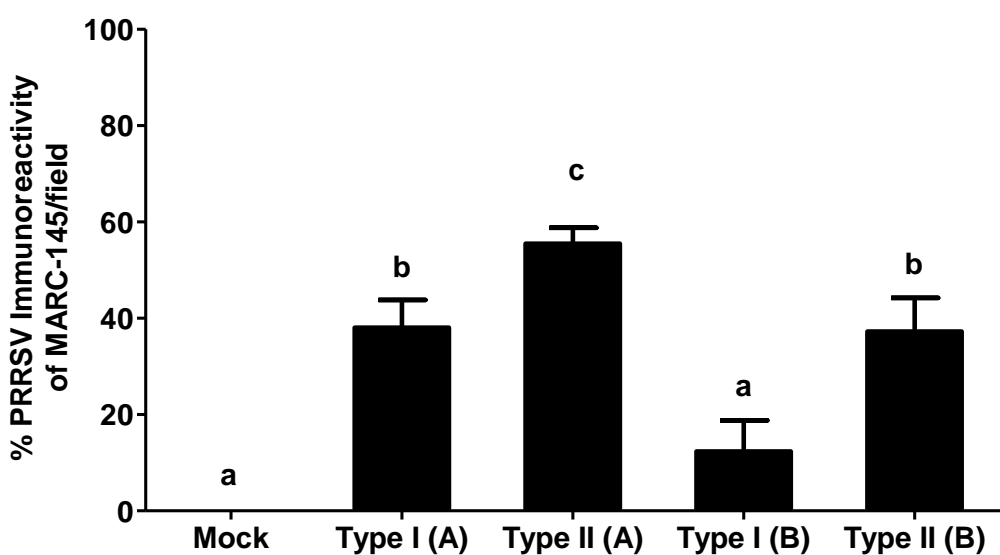
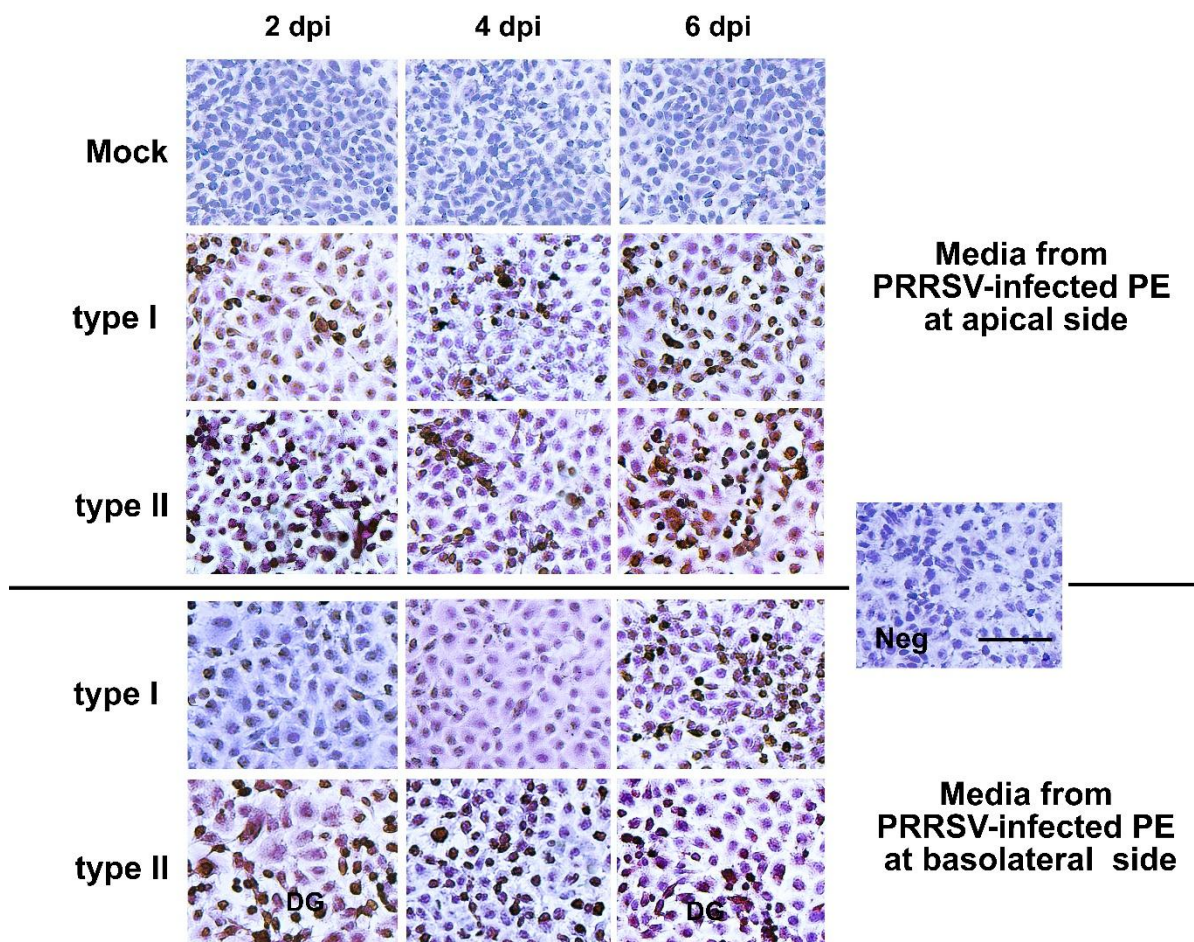


Figure 4 Detection of PRRSV in MARC-145 cells inoculated with a culture medium of PRRSV-infected PE cells at 2, 4 and 6 dpi. Following apical or basolateral with PRRSV (type I or type II) for 1 h., culture media from both sides of PE cells grown on microporous membrane were collected to inoculate MARC-145 cells. The upper panel shows immunocytochemistry staining of anti PRRSV-GP5 antibody in dark-brown color, and CPE in PRRSV inoculated MARC-145 cells. DG=degeneration. Scale bar = 500 μ m. The lower panel bar graph shows mean \pm SEM of % PRRSV immunoreactivity/field in MARC-145 cells inoculated with culture media from type I or type II PRRSV-infected PE cells at (A) apical side or at (B) basolateral side observed at 2, 4 and 6 dpi (n = 5 pigs). Bar graph with different letters (a, b or c) indicates significant difference at $p < 0.05$ by one-way ANOVA followed by Newman-Kuel post-hoc test.

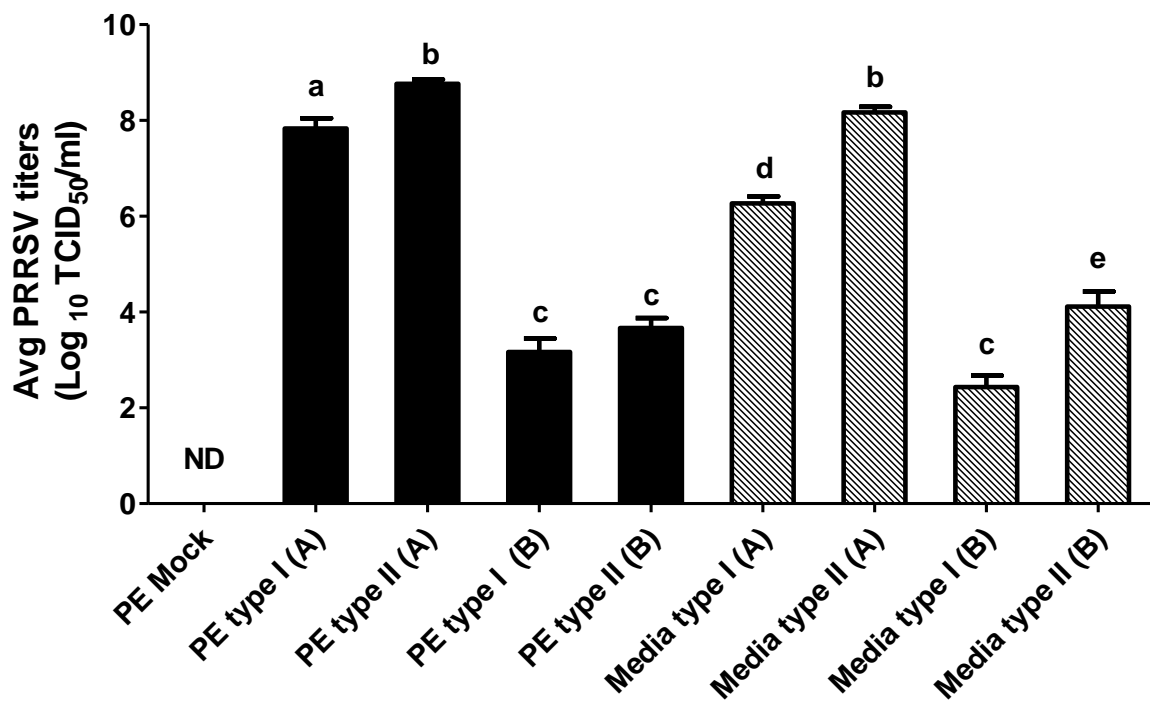


Figure 5 Comparison of the overall PRRSV production in the PRRSV-inoculated PE cells and their culture media. PRRSV infected PE cells and culture supernatant collected at 2, 4 and 6 dpi were analyzed virus titers by Reed and Muench calculation of the CPE in tissue culture 50% endpoint (TCID₅₀/ml). Bar graph represents mean \pm SEM of the average viral titers in \log_{10} TCID₅₀/ml (n = 5 pigs) observed at 2, 4 and 6 dpi. Bar graph with different letters (a, b, c, d or e) indicates significant difference at $p < 0.05$ by one-way ANOVA followed by Newman-Kuel post-hoc test.

Changes of Tissue Epithelial Resistance (TER) and Potential Difference (PD) in response to PRRSV inoculation: To test whether PRRSV infection directly affected the epithelial membrane integrity of PE cells, an EVOM was employed to detect changes in TER and PD every two days prior to immunocytochemistry and CPE performance. As shown in table 1, only PRRSV type I or II inoculation at the apical side of the epithelial monolayer induced the changes of TER in a similar manner to normal or the mock. In mock inoculated PE cells, TER and PD gradually increased by 10-20% every two days. In contrast, the TER of PE cells inoculated with PRRSV type II was not changed from the initial value (Table 1). Additionally, the PD values of both type I and type II-inoculated cells showed no significant changes from the control mock at any dpi.

Discussion

Infection by PRRSV is limited to some kinds of cells due to the very narrow tropism of PRRSV. PRRSV tropism is explained by the cell allowing viral particles to attach and continue with multiple steps including distribution through the host cell membrane, binding to receptors, viral entry and releasing the viral genome for subsequent viral replication (Maginnis, 2018). Macrophage and monocyte lineages have been reported as natural targets of PRRSV (Duan et al., 1997; Teifke et al., 2001), since they express PRRSV specific receptors CD163 and sialoadhesin (Sn). Apart from natural inoculation in macrophages and monocytes, some cell lines such as CL2621, MA-104, and MARC-145 cells have been reported to be PRRSV-permissive

cells (Benfield et al., 1992; Bautista et al., 1993; Kim et al., 1993). The present study is the first to demonstrate that porcine glandular endometrial cells (PE) are additional targets for direct susceptibility to PRRSV infection.

Under basal conditions without PRRSV infection, PE cells express high levels of ER- α and - β receptor proteins. This confirms that the PE cell monolayer is of endometrial epithelial origin and can be a target of estrogens, which is considered as a feto-placental membrane and site of PRRSV infection (Karniychuk and Nauwynck, 2013). In agreement with the previous *in vivo* study, little expression of CD163 or Sn was observed in non-inoculated PE cells. However, porcine endometrial endothelial cells which can be susceptible to PRRSV have been found to express only Sn and the other PRRSV mediators i.e. CD151 (Feng et al., 2013). These endothelial cells surrounding the placenta have been indicated as associated with reproductive failure in PRRSV-infected sows (Feng et al., 2013). In our study, PE cells which were characterized as CD163-Sn-cells could be susceptible to PRRSV as evidenced by the presence of CPE and PRRSV-GP5 expression following PRRSV infection. Perhaps, CD151 the other adhesion molecules, or pathogen recognition receptors (PRRs), i.e. toll-like receptors (TLR)3, TLR7 or TLR9 that can recognize structural proteins at the envelope and nucleocapsids of PRRSV in macrophages might be accompanied and employed for PRRSV infection (Kuzemtseva et al., 2014; Bhella, 2015).

Table 1 Effects of PRRSV inoculation on the electrical properties of PE cells. Value represents mean \pm SEM of tissue epithelial resistance (TER) or tissue potential difference (PD) value measured at 0, 2, 4 and 6 dpi in triplicate. * or ** indicates the significant differences at p value <0.05 or <0.01 from 0 dpi by one-way ANOVA followed by Dunnert post-hoc test.

	Tissue Epithelial Resistance (TER; Ohm.cm ²)				Tissue Potential Difference (PD; mVolts)			
	0 dpi	2 dpi	4 dpi	6 dpi	0 dpi	2 dpi	4 dpi	6 dpi
<i>Apical inoculation</i>								
Mock	546.67 \pm 18.40	583.00 \pm 7.79	666.50 \pm 31.16	673.50 \pm 9.34	46.27 \pm 1.56	60.03 \pm 1.85	74.40 \pm 5.11	66.92 \pm 5.27
PRRSV type I	525.83 \pm 10.10	573.72 \pm 16.64	571.63 \pm 8.41	593.83 \pm 18.19	40.89 \pm 2.71	46.81 \pm 2.71	62.57 \pm 3.54	58.08 \pm 5.88
PRRSV type II	532.06 \pm 17.35	540.94 \pm 23.92	541.56 \pm 22.95**	572.25 \pm 8.72*	39.97 \pm 2.78	48.87 \pm 2.43	59.75 \pm 4.90	54.53 \pm 4.50
<i>Basolateral inoculation</i>								
Mock	573.50 \pm 11.26	595.25 \pm 11.26	682.00 \pm 46.77	658.75 \pm 0.72	46.95 \pm 2.08	59.75 \pm 2.26	73.13 \pm 6.08	66.25 \pm 6.49
PRRSV type I	542.11 \pm 6.85	620.00 \pm 25.96	619.88 \pm 11.34	616.00 \pm 21.35	43.47 \pm 3.76	59.17 \pm 2.76	70.00 \pm 3.27	67.28 \pm 6.36
PRRSV type II	548.72 \pm 8.94	556.78 \pm 30.18	593.56 \pm 12.35*	616.42 \pm 19.16	41.66 \pm 3.93	54.02 \pm 3.34	60.30 \pm 6.18	61.86 \pm 5.78

An additional aspect of viral infection via uterine lumen or blood circulation is of interest. In the present study, PE cell monolayers were cultured in permeable membrane to compare the effects between two routes of infection (apical and basolateral). Basolateral infection simulates the transmission of PRRSV from blood circulation to endometrial cells, while apical infection refers to PRRSV transmission from fetus to dam. Our findings showed that higher CPE occurrence was apparent in PE cells apically inoculated with either type I or II PRRSV. Moreover, PRRSV-GP5 positive cells were detected in PE cells after apical, but not basolateral, inoculation with type I or type II PRRSV. These observations suggest that the route of PRRSV entry is important for the persistence of PRRSV. It appears that transmission of PRRSV from fetus to dam may be the predominate site of PRRSV infection.

Different PRRSV genotypes have been demonstrated to relate with different severity and clinical outcome (Nelsen *et al.*, 1999). PRRSV type II infection causes more severe respiratory distress than type I (Nielsen *et al.*, 2002); however, both genotypes cause reproductive failure to the same degree (Scortti *et al.*, 2006). Our current results showed that CPE, PRRSV positive of PE cells and viral load produced by type II were greater than those by type I, which is in agreement with natural infection or *in vivo* study (Ladinig *et al.*, 2015). In that study, PRRSV type II could not demonstrate the virulence of reproductive signs, i.e. viral load in the fetus or maternal-fetal interface, numbers of embryonic death or PRRSV-positive litters, that differ from type I (Ladinig *et al.*, 2015). Perhaps, in the uterus, the determinant of distinct virulence between type I and type II infection appears to depend upon viral protein expression, such as non-structural glycoproteins (Nsp 3-8) and host interaction during viral replication (Kwon *et al.*, 2008).

The PRRSV that transmitted into PE cells were not only presumably replicated, but also released into surrounding compartment. This was supported by the findings that MARC-145 cells incubated with culture media collected from apical and/or basolateral compartments of the PRRSV-infected PE cells were positive to PRRSV proteins and contained copies of viral nucleic acid ($\geq 10^2$ TCID₅₀/ml). Nevertheless, the present study could not show the kinetics of viral production, expression and CPE at each time point since the pattern of viral load, i.e. onset and peak of viral load had variation among primary porcine uterine tissue culture. For this reason, the overall results of viral titers, %PRRSV immunoreactivity and %CPE generated by PRRSV inoculum during 2, 4 and 6 dpi were compared among groups, which may be suitable for this study model using primary cell culture. These results suggest the advantage of the recent PE cell model to propagate the viral progeny. However, the possibility of PE cells to be phenotypically stable and yield high titers of progeny virus needs to be further investigated.

When focussing on the examining of PRRSV infected-PE cells as the viral spreading site, supernatant samples from both apical and basolateral component of all infected PE cells contained PRRSV copies indicated by MARC-145 infectivity study. Even though, supernatant of basolateral PRRSV-infected PE

cells consisted of viral copies less than those of apical infection, we could not assume that the apical route had more significance in the transmission of PRRSV infection than the basolateral route (Fig. 5). These released PRRSV seem to be virulent as virus isolation from the field, since PRRSV released from basolateral but not apical infection in PE cell produced CPE in MARC-145. Possibly, the basolateral membrane presents a structure that impedes PRRSV entry (Bomsel and Alfsen, 2003). PRRSV may adhere to the membrane of the PE cell, but not translocate or replicate within PE cell. However, the adhered PRRSV may be released into the surrounding vicinity. Furthermore, the released PRRSV in continuing to the surrounded PRRSV-contaminant PE cell monolayers may concur to the evidence that naïve sows primarily exposed to PRRSV can be long-lastingly transmitted PRRSV to herds. Nevertheless, whether or not the released PRRSV from PE cells could come across the natural impediment, such as muscular layers or connective tissues to the fetus, requires further investigation.

In the other viral infection preference to the apical surface, such as respiratory syncytial virus (RSV), it usually produces a serious inflammatory response to facilitate the bacterial colonization at the apical surface of airway epithelium (Bousquet *et al.*, 2000; Singh *et al.*, 2007). In the present study, the decreased TER or PD reflecting a loosening of tight junction barrier properties could not be observed in PRRSV-infected cell, even though the characteristics of these cells were different from the mocks or normal PE cells. In general, during *in vitro* culture of monolayer cells including PE cells, an increase in TER and a decrease in paracellular permeability was induced by series of growth factors in cell culture medium (Podolsky, 1993; Deachapunya and O'Grady, 1998). The proliferation of epithelial cell associated with more cytoskeletal proteins, such as cytokeratin 18 and tight junction forming have been suggested as the underlying mechanism (Podolsky, 1993). It is speculated that PRRSV-host interaction at the apical aspects of endometrial epithelium may inhibit cell proliferation or induce cell death. The apoptotic cells induced by PRRSV could account for the results as has been evidenced in cells at the fetal implantation site of PRRSV-infected sows (Karniychuk *et al.*, 2011). Even though the cell death and apoptosis were not evaluated, the observation of degenerative cells in the PRRSV-infected PE cells associated with low TER in this study could indicate the PRRSV induced PE cell injury. These situations may disturb the placenta function in nourishing and protecting the embryo and fetus, which may be the consequence of reproductive failure in PRRSV infection. It will be of interest to study further, whether the interactions can extend to PE cells co-cultured with macrophages, which naturally simulate the pathogenesis of PRRSV spreading from infected endometrial macrophages to the uterine epithelium.

In conclusion, porcine endometrial cells are one of the targets that can be directly infected with PRRSV. The findings may provide an alternative consideration for PRRSV-induced reproductive failure and be associated to the re-circulation of PRRSV in herds. Furthermore, these cells deserve to be an additional

model for studying the underlying mechanisms of PRRSV-induced reproductive failure.

Acknowledgements

This work was supported by research grants from Chulalongkorn University (CU-56-644-HR and GRB_BSS_73_58_31_04); the 90th and 100th Anniversary of Chulalongkorn University Fund (Ratchadapiseksomphot Endowment Fund GCUGR1125604041D/2560) awarded to Sutthasinee Poonyachoti and Muttarin Lothong. We wish to thank Dran Rukarcheep for his assistance in this study.

References

Bautista EM, Goyal SM, Yoon IJ, Joo HS and Collins JE 1993. Comparison of porcine alveolar macrophages and CL 2621 for the detection of porcine reproductive and respiratory syndrome (PRRS) virus and anti-PRRS antibody. *J Vet Diagn Invest.* 5(2): 163-165.

Benfield DA, Nelson E, Collins JE, Harris L, Goyal SM, Robison D, Christianson WT, Morrison RB, Gorcyca D and Chladek D 1992. Characterization of swine infertility and respiratory syndrome (SIRS) virus (isolate ATCC VR-2332). *J Vet Diagn Invest.* 4(2): 127-133.

Bhella D 2015. The role of cellular adhesion molecules in virus attachment and entry. *Philosophical Transactions of the Royal Society B: Biological Sciences.* 370(1661): 20140035.

Bomsel M and Alfsen A 2003. Entry of viruses through the epithelial barrier: pathogenic trickery. *Nat Rev Mol Cell Biol.* 4: 57.

Bousquet J, Jeffery PK, Busse WW, Johnson M and Vignola AM 2000. Asthma: from bronchoconstriction to airways inflammation and remodeling. *Am J Respir Crit Care Med.* 161(5): 1720-1745.

Caselli E, Bortolotti D, Marci R, Rotola A, Gentili V, Soffritti I, D'Accolti M, Lo Monte G, Sicolo M, Barao I, Di Luca D and Rizzo R 2017. HHV-6A Infection of Endometrial Epithelial Cells Induces Increased Endometrial NK Cell-Mediated Cytotoxicity. *Front Microbiol.* 8: 2525.

Deachapunya C and O'Grady SM 1998. Regulation of chloride secretion across porcine endometrial epithelial cells by prostaglandin E2. *J Physiol.* 508 (Pt 1): 31-47.

Ding Z, Li ZJ, Zhang XD, Li YG, Liu CJ, Zhang YP and Li Y 2012. Proteomic alteration of Marc-145 cells and PAMs after infection by porcine reproductive and respiratory syndrome virus. *Vet Immunol Immunopathol.* 145(1-2): 206-213.

Dokland T 2010. The structural biology of PRRSV. *Virus Res.* 154(1-2): 86-97.

Donofrio G, Ravanetti L, Cavarani S, Herath S, Capocefalo A and Sheldon IM 2008. Bacterial infection of endometrial stromal cells influences bovine herpesvirus 4 immediate early gene activation: a new insight into bacterial and viral interaction for uterine disease. *Reproduction.* 136(3): 361-366.

Duan X, Nauwynck HJ and Pensaert MB 1997. Virus quantification and identification of cellular targets in the lungs and lymphoid tissues of pigs at different time intervals after inoculation with porcine reproductive and respiratory syndrome virus (PRRSV). *Vet Microbiol.* 56(1-2): 9-19.

Feng L, Zhang X, Xia X, Li Y, He S and Sun H 2013. Generation and characterization of a porcine endometrial endothelial cell line susceptible to porcine reproductive and respiratory syndrome virus. *Virus Res.* 171(1): 209-215.

Filant J and Spencer TE 2014. Uterine glands: biological roles in conceptus implantation, uterine receptivity and decidualization. *Int J Dev Biol.* 58(2-4): 107-116.

Frydas IS, Verbeeck M, Cao J and Nauwynck HJ 2013. Replication characteristics of porcine reproductive and respiratory syndrome virus (PRRSV) European subtype 1 (Lelystad) and subtype 3 (Lena) strains in nasal mucosa and cells of the monocytic lineage: indications for the use of new receptors of PRRSV (Lena). *Vet Res.* 44(1): 73-73.

Karniychuk UU and Nauwynck HJ 2009. Quantitative changes of sialoadhesin and CD163 positive macrophages in the implantation sites and organs of porcine embryos/fetuses during gestation. *Placenta.* 30(6): 497-500.

Karniychuk UU and Nauwynck HJ 2013b. Pathogenesis and prevention of placental and transplacental porcine reproductive and respiratory syndrome virus infection. *Vet Res.* 44(1): 95.

Karniychuk UU, Saha D, Geldhof M, Vanhee M, Cornillie P, Van den Broeck W and Nauwynck HJ 2011. Porcine reproductive and respiratory syndrome virus (PRRSV) causes apoptosis during its replication in fetal implantation sites. *Microb Pathog.* 51(3): 194-202.

Kim HS, Kwang J, Yoon IJ, Joo HS and Frey ML 1993. Enhanced replication of porcine reproductive and respiratory syndrome (PRRS) virus in a homogeneous subpopulation of MA-104 cell line. *Arch Virol.* 133(3-4): 477-483.

Kuzemtseva L, de la Torre E, Martín G, Soldevila F, Ait-Ali T, Mateu E and Darwich L 2014. Regulation of toll-like receptors 3, 7 and 9 in porcine alveolar macrophages by different genotype 1 strains of porcine reproductive and respiratory syndrome virus. *Vet Immunol Immunopathol.* 158(3): 189-198.

Kwon B, Ansari IH, Pattnaik AK and Osorio FA 2008. Identification of virulence determinants of porcine reproductive and respiratory syndrome virus through construction of chimeric clones. *Virology.* 380(2): 371-378.

Ladinig A, Detmer SE, Clarke K, Ashley C, Rowland RR, Lunney JK and Harding JC 2015. Pathogenicity of three type 2 porcine reproductive and respiratory syndrome virus strains in experimentally inoculated pregnant gilts. *Virus Res.* 203: 24-35.

Liu J-K, Wei C-H, Yang X-Y, Dai A-L and Li X-H 2013. Multiplex PCR for the simultaneous detection of porcine reproductive and respiratory syndrome virus, classical swine fever virus, and porcine circovirus in pigs. *Mol Cell Probes.* 27(3-4): 149-152.

Lorenzen E, Follmann F, Jungersen G and Agerholm JS 2015. A review of the human vs. porcine female genital tract and associated immune system in the perspective of using minipigs as a model of human genital Chlamydia infection. *Vet Res.* 46: 116.

Maginnis MS 2018. Virus-Receptor Interactions: The Key to Cellular Invasion. *J Mol Biol.* 430(17): 2590-2611.

Meng XJ, Paul PS, Halbur PG and Lum MA 1996. Characterization of a high-virulence US isolate of porcine reproductive and respiratory syndrome virus in a continuous cell line, ATCC CRL11171. *J Vet Diagn Invest.* 8(3): 374-381.

Nelsen CJ, Murtaugh MP and Faaberg KS 1999. Porcine reproductive and respiratory syndrome virus comparison: divergent evolution on two continents. *J Virol.* 73(1): 270-280.

Nielsen J, Botner A, Bille-Hansen V, Oleksiewicz MB and Storgaard T 2002. Experimental inoculation of late term pregnant sows with a field isolate of porcine reproductive and respiratory syndrome vaccine-derived virus. *Vet Microbiol.* 84(1-2): 1-13.

Podolsky DK 1993. Regulation of intestinal epithelial proliferation: a few answers, many questions. *Am J Physiol Gastrointest Liver Physiol.* 264(2): G179-G186.

Reed L and Muench H 1938. A simple method of estimating fifty percent endpoints.(1938). *The American Journal of Hygiene* (27). 493-497.

Rosso KD, Laube KL, Goyal SM and Collins JE 1996. Fetal microscopic lesions in porcine reproductive and respiratory syndrome virus-induced abortion. *Vet Pathol.* 33(1): 95-99.

Scortti M, Prieto C, Martinez-Lobo FJ, Simarro I and Castro JM 2006. Effects of two commercial European modified-live vaccines against porcine reproductive and respiratory syndrome viruses in pregnant gilts. *Vet J.* 172(3): 506-514.

Singh D, McCann KL and Imani F 2007. MAPK and heat shock protein 27 activation are associated with respiratory syncytial virus induction of human bronchial epithelial monolayer disruption. *Am J Physiol Lung Cell Mol Physiol.* 293(2): L436.

Snijder EJ and Meulenberg JJ 1998. The molecular biology of arteriviruses. *J Gen Virol.* 79 (Pt 5): 961-979.

Teifke JP, Dauber M, Fichtner D, Lenk M, Polster U, Weiland E and Beyer J 2001. Detection of European porcine reproductive and respiratory syndrome virus in porcine alveolar macrophages by two-colour immunofluorescence and in-situ hybridization-immunohistochemistry double labelling. *J Comp Pathol.* 124(4): 238-245.

Van Breedam W, Van Gorp H, Zhang JQ, Crocker PR, Delputte PL and Nauwynck HJ 2010. The M/GP(5) Glycoprotein Complex of Porcine Reproductive and Respiratory Syndrome Virus Binds the Sialoadhesin Receptor in a Sialic Acid-Dependent Manner. *PLoS Path.* 6(1): e1000730.